
Breaking Information Cocoons: A Hyperbolic Graph-LLM Framework for Exploration and Exploitation in Recommender Systems

Qiyao Ma¹ Menglin Yang^{†2} Mingxuan Ju^{*3} Tong Zhao^{*3} Neil Shah^{*3} Rex Ying²

Abstract

Modern recommender systems often create information cocoons, restricting users’ exposure to diverse content. A key challenge lies in balancing content exploration and exploitation while allowing users to adjust their recommendation preferences. Intuitively, this balance can be modeled as a tree-structured representation, where depth search facilitates exploitation and breadth search enables exploration. However, existing approaches face two fundamental limitations: Euclidean methods struggle to capture hierarchical structures, while hyperbolic methods, despite their superior hierarchical modeling, lack semantic understanding of user and item profiles and fail to provide a principled mechanism for balancing exploration and exploitation. To address these challenges, we propose HERec, a hyperbolic graph-LLM framework that effectively balances exploration and exploitation in recommender systems. Our framework introduces two key innovations: (1) a hierarchical-aware graph-LLM mechanism that jointly aligns textual descriptions with user-item collaborative information in hyperbolic space, and (2) a hierarchical representation structure that enables user-adjustable exploration-exploitation trade-offs. Extensive experiments demonstrate that HERec consistently outperforms both Euclidean and hyperbolic baselines, achieving up to 5.49% improvement in utility metrics and 11.39% increase in diversity metrics, effectively mitigating information cocoons.

1. INTRODUCTION

As online platforms grow in size dramatically, users are overwhelmed by an influx of information, creating informa-

tion cocoons that restrict their exposure to diverse and novel content (Kunaver & Požrl, 2017; Castells et al., 2021).

Traditional recommendation approaches have primarily relied on collaborative filtering and interaction data (He et al., 2020; Koren et al., 2009), where users with similar historical preferences are expected to share future interests (Chen et al., 2021). However, these methods face two critical challenges in improving user experience. First, existing models struggle to capture the underlying hierarchical structure inherent in user-item networks (Zheng et al., 2017; Unger & Tuzhilin, 2020), a critical factor for enhancing performance and personalization. Second, these models fail to effectively balance the exploration-exploitation trade-off. For instance, a jazz enthusiast may want to explore rock music, but current models primarily focus on exploitation—recommending only familiar genres—without adequately supporting exploration (as illustrated in Figure 1).

Hyperbolic space has emerged as a promising approach for modeling hierarchical structures and power-law distributions (Krioukov et al., 2010; Yang et al., 2022b; Sun et al., 2021; Yang et al., 2022a), where its exponential volume growth naturally aligns with hierarchical, scale-free structures (Ganea et al., 2018; Chami et al., 2019; Liu et al., 2019; Zhang et al., 2021; Yang et al., 2023). In hyperbolic space, distances increase exponentially from the origin, allowing popular items or exploratory users to be positioned closer to the origin, while niche items or users with focused interests spread toward the boundaries. This spatial configuration enables hyperbolic graph neural network (GNN) models to perceive hierarchical relationships effectively, enhancing recommendation performance (Yang et al., 2022a; Sun et al., 2021; Yang et al., 2022b).

Despite these advantages, current hyperbolic recommender systems still face key limitations. First, they struggle with a lack of semantic understanding of user and item profiles. While large language models (LLMs) offer a potential solution, their text encoders operate in Euclidean space, making it challenging to integrate LLM-derived semantic features with hyperbolic collaborative signals. This mismatch leaves existing hyperbolic models vulnerable to noise in collaborative information, as they fail to capture semantic insights effectively. Second, hyperbolic recommender systems lack

¹The University of Hong Kong ²Yale University ³Snap Inc.. Correspondence to: Menglin Yang[†] <mlyang.yale@outlook.com>. ^{*}Authors affiliated with Snap Inc. served in advisory roles only for this work.

a principled approach to balancing exploration (introducing new content) and exploitation (focusing on existing preferences) (Wilson et al., 2021). This limitation reduces their ability to adapt to the exploration-exploitation trade-off, ultimately diminishing both the utility and diversity of recommendations.

Proposed Methods. To address these challenges, we propose HERec, a hyperbolic graph-LLM framework designed to balance exploration and exploitation in recommender systems. Our approach introduces two key innovations: (1) a hierarchical-aware graph-LLM alignment mechanism, which jointly aligns textual descriptions with user-item collaborative information in hyperbolic space, supported by theoretical gradient analysis demonstrating its advantages, and (2) a novel hierarchical representation structure that enables user-adjustable exploration-exploitation trade-offs. Unlike conventional approaches that require manually defined hierarchies, we propose a hyperparameter-free clustering mechanism theoretically optimized by Dasgupta’s cost (Dasgupta, 2016). This approach automatically discovers hierarchical structures without requiring predefined hyperparameters, allowing for a more adaptive and principled organization of user preferences.

To validate the effectiveness of HERec, we conducted extensive experiments across multiple dimensions. Our model consistently outperformed baselines in both utility and diversity metrics, marking a significant achievement as it is the first model to excel in both aspects simultaneously. For a fair comparison, we enhanced Euclidean baselines with feature information, yet our model still demonstrated superior performance, validating the advantage of our designed alignment in hyperbolic space. Additionally, we conducted a detailed analysis on head and tail items, showing that HERec effectively boosts recommendations for tail items, thus enhancing diversity. An ablation study, along with a hierarchical representation structure analysis and decoder module, confirms HERec’s capability to leverage both semantic meaning and collaborative information, providing deeper insights into the advantages of our approach.

Contributions. Our primary contributions focus on three key aspects: capturing collaborative signals, integrating semantic information, and modeling the underlying hierarchical structure. The proposed graph-LLM alignment framework unifies collaborative and semantic information in hyperbolic space, while a hierarchical representation structure organizes user preferences, allowing for dynamic adjustment between exploration and exploitation. Moreover, through extensive experiments, we demonstrate that HERec achieves state-of-the-art performance across both utility and diversity metrics, making it the first model to excel in both criteria simultaneously. To facilitate reproducibility and further research, we open-source our model implementation

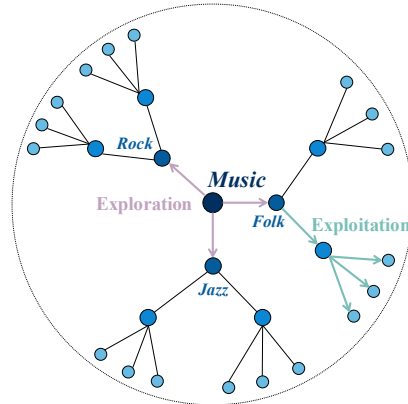


Figure 1. Exploration and exploitation in hyperbolic space.

at: <https://github.com/Martin-qyma/HERec>.

2. Related Work

In this section, we review graph-based collaborative filtering, large language models (LLMs) for recommendation, and hyperbolic representation learning methods.

Graph Collaborative Filtering. Graph Collaborative Filtering has emerged as a dominant approach in recommender systems, with graph neural networks (GNNs) playing a central role. Unlike traditional collaborative filtering techniques, such as matrix factorization (Koren et al., 2009), GNNs capitalize on the relational structure in user-item interactions, enabling a more nuanced understanding of complex dependencies. Prominent graph-based methods, such as NGCF (Wang et al., 2019), SGL (Wu et al., 2021), and LightGCN (He et al., 2020), have been widely adopted and have consistently achieved state-of-the-art performance. Nevertheless, these models are constrained to Euclidean space, which may fall short in capturing the underlying power-law distribution in user-item networks.

Large Language Models for Recommendation. Large language models (LLMs) are increasingly used in recommender systems for their strong capability in understanding textual information. Some approaches leverage LLMs directly for downstream recommendation tasks (Bao et al., 2023; Li et al., 2023; Lyu et al., 2023; Zheng et al., 2024; Zhang et al., 2023), while others utilize LLMs as an auxiliary tool for collaborative filtering (Ren et al., 2024; Xi et al., 2024; Wei et al., 2024). However, these approaches require substantial inference time and are computationally inefficient. In our HERec, we use language models exclusively to improve data quality, eliminating the need for repeated inference during each recommendation by utilizing hyperbolic embeddings for the final output.

Hyperbolic Representation Learning. To address the limitations of Euclidean space in modeling hierarchical structures, researchers have investigated the use of hyperbolic

space (Chami et al., 2019; Liu et al., 2019; Yang et al., 2022b; Zhang et al., 2021), where distances grow exponentially as embeddings move away from the origin. This property makes hyperbolic geometry particularly well-suited for modeling user-item interactions by more accurately capturing latent hierarchies and dependencies. Consequently, hyperbolic representation learning has gained considerable attention in the recommender systems domain (Ying et al., 2018; Vinh Tran et al., 2020; Sun et al., 2021; Yang et al., 2022a), demonstrating improved performance over traditional Euclidean models.

However, none of these hyperbolic models fully leverage the rich semantic information embedded in language-based datasets. While some approaches incorporate knowledge graphs as supplementary information (Tai et al., 2021; Du et al., 2022), these models primarily focus on refining hierarchical structures rather than achieving a deeper semantic understanding of each item or user.

3. PRELIMINARIES

Embeddings learned from graph collaborative filtering are by default in the Euclidean space, which is unable to capture tree-like structures. To address the problem, we introduce how to derive these embeddings in a hyperbolic space.

Riemannian Manifold. A Riemannian manifold (\mathcal{M}, g) is a smooth manifold that features an inner product $g_x : T_x\mathcal{M} \times T_x\mathcal{M} \rightarrow \mathbb{R}$ at each point $x \in \mathcal{M}$. This inner product, known as the Riemannian metric, defines geometric characteristics of the space such as angles and curve lengths. The curvature of Riemannian manifolds results in different types of geometries: elliptic geometry with positive curvature, Euclidean geometry with zero curvature, and hyperbolic geometry with negative curvature. In this work, we focus on hyperbolic geometry, characterized by negative curvature. Hyperbolic space can be described by several equivalent models, each offering unique properties while being mathematically equivalent. The Lorentz model, also referred to as the hyperboloid model, is one of the commonly used representations of hyperbolic space.

Lorentz Model. An n -dimensional Lorentz manifold with negative curvature $-1/\kappa$ ($\kappa > 0$) is described as the Riemannian manifold $(\mathbb{H}_\kappa^n, g_\mathcal{L})$. Here, $\mathbb{H}_\kappa^n = \{x \in \mathbb{R}^{n+1} : \langle x, x \rangle_\mathcal{L} = -\kappa, x_0 > 0\}$, $g_\mathcal{L} = \eta$ with $\eta = \mathbf{I}_n$ except $\eta_{0,0} = -1$, and $\langle \cdot, \cdot \rangle_\mathcal{L}$ represents the Lorentzian inner product, which is defined

$$\langle x, y \rangle_\mathcal{L} := -x_0y_0 + \sum_{i=1}^n x_iy_i \quad (1)$$

A tangent space is an n -dimensional vector space that approximates Euclidean space to hyperbolic space. Specifically, given a point $x \in \mathbb{H}_\kappa^n$, there exists a tangent space

$\mathcal{T}_x\mathbb{H}_\kappa^n$ that approximates \mathbb{H}_κ^n :

$$\mathcal{T}_x\mathbb{H}_\kappa^n := \{v \in \mathbb{R}^{n+1} : \langle v, x \rangle_\mathcal{L} = 0\} \quad (2)$$

We also need to define transitions between \mathbb{H}_κ^n and $\mathcal{T}_x\mathbb{H}_\kappa^n$, which give rise to the exponential and logarithmic maps. For $x \in \mathbb{H}_\kappa^n$ and $v \in \mathcal{T}_x\mathbb{H}_\kappa^n$ with $v \neq \mathbf{0}$ and $y \neq x$, there exists a unique geodesic $\gamma : [0, 1] \rightarrow \mathbb{H}_\kappa^n$ such that $\gamma(0) = x$ and $\gamma'(0) = v$. The exponential map $\exp_x : \mathcal{T}_x\mathbb{H}_\kappa^n \rightarrow \mathbb{H}_\kappa^n$ is given by $\exp_x(v) = \gamma(1)$:

$$\exp_x^\kappa(v) = \cosh\left(\frac{\|v\|_\mathcal{L}}{\sqrt{\kappa}}\right)x + \sqrt{\kappa} \sinh\left(\frac{\|v\|_\mathcal{L}}{\sqrt{\kappa}}\right) \frac{v}{\|v\|_\mathcal{L}} \quad (3)$$

where $\|v\|_\mathcal{L} = \sqrt{\langle v, v \rangle_\mathcal{L}}$ denotes the Lorentzian norm of v . The logarithmic map \log_x is the inverse of the exponential map \exp_x , and the distance between x and y in \mathbb{H}_κ^n is:

$$\log_x^\kappa(y) = d_\mathcal{L}^\kappa(x, y) \frac{y + \frac{1}{\kappa}\langle x, y \rangle_\mathcal{L}x}{\|y + \frac{1}{\kappa}\langle x, y \rangle_\mathcal{L}x\|} \quad (4)$$

where $d_\mathcal{H}^\kappa(x, y)$ is the distance between x and y in \mathbb{H}_κ^n :

$$d_\mathcal{H}^\kappa(x, y) = \sqrt{\kappa} \operatorname{arccosh}(-\langle x, y \rangle_\mathcal{L}/\kappa) \quad (5)$$

We choose $\mathbf{o} := \{\sqrt{\kappa}, 0, \dots, 0\} \in \mathbb{H}_\kappa^n$ as the reference point for all the operations, making the transitions reproducible. In this work, we set $\kappa = 1$, resulting in a curvature of -1 . Therefore, in the following discussions, we would omit κ for simplicity.

4. METHODOLOGY

In this section, we present a comprehensive overview of our proposed model, HERec. Our approach not only aims to deliver accurate recommendations but also addresses users' growing demand for more diverse suggestions. Furthermore, by constructing a hierarchical tree from the learned embeddings, we introduce an additional mechanism that enables users to control the degree of exploration in the recommended items. The overall framework is in Figure 2.

4.1. Hyperbolic Graph Collaborative Filtering

Similar to Euclidean space, hyperbolic graph collaborative filtering captures user-item dependencies via message passing mechanism. In our method, we use the Lorentz representation for both users and items.

Hyperbolic Embedding Initialization. As discussed in section 3, we fix the origin $\mathbf{o} := \{\sqrt{\kappa}, 0, \dots, 0\} \in \mathbb{H}_\kappa^n$ and use it as the reference point. We adopt the Gaussian sampling method for the initialization of embeddings in Euclidean space, after that, by injecting them into the tangent space of the reference point, we derive the initial hyperbolic embed-

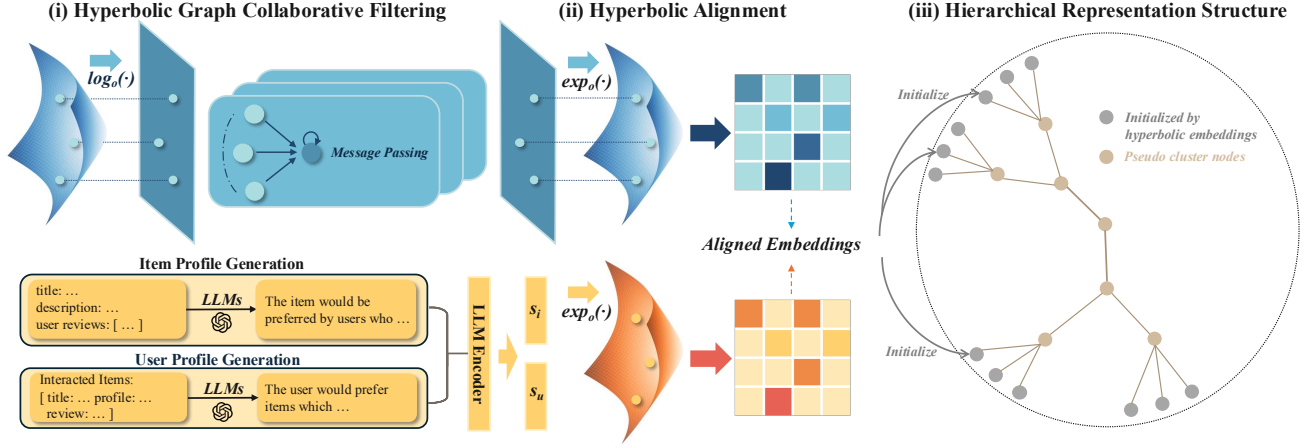


Figure 2. The overall architecture of HERec. (i) Hyperbolic Graph Collaborative Filtering: Encodes collaborative information using hyperbolic GNNs; (ii) Hyperbolic Alignment: Aligns semantic and collaborative information within hyperbolic space; (iii) Hierarchical Representation Structure: Builds hierarchy structure from hyperbolic embeddings.

dings of both users and items:

$$\begin{aligned} z_u^0 &= (0, e_u), & z_i^0 &= (0, e_i) \\ h_u^0 &= \exp_{\circ}(z_u^0), & h_i^0 &= \exp_{\circ}(z_i^0) \end{aligned} \quad (6)$$

where e_u, e_i are Gaussian distributed initialized Euclidean embeddings, and z_u^0, z_i^0 are corresponding embeddings in the tangent space of the origin point. h_u^0, h_i^0 therefore stands for the resulting initialized hyperbolic embeddings.

Hyperbolic Message Passing. Message passing between each node is realized through hyperbolic neighborhood aggregation, which is used to extract explicit user-item interaction. Given user u , item i , as well as their neighborhood $\mathcal{N}_u, \mathcal{N}_i$, their embeddings at layer l in the tangent space are updated as follows:

$$z_u^l = z_u^{l-1} + \sum_{i \in \mathcal{N}_u} \frac{1}{|\mathcal{N}_u|} z_i^{l-1}, \quad z_i^l = z_i^{l-1} + \sum_{u \in \mathcal{N}_i} \frac{1}{|\mathcal{N}_i|} z_u^{l-1} \quad (7)$$

where $|\mathcal{N}_u|$ and $|\mathcal{N}_i|$ represent the number of neighbors of u and i , respectively. The final tangent space embedding is derived by summing up embeddings at each layer:

$$z_u = \sum_l z_u^l, \quad z_i = \sum_l z_i^l \quad (8)$$

Since z_u and z_i are on the tangent space, we still need to project it into hyperbolic space to derive the hyperbolic embeddings:

$$h_u = \exp_{\circ}(z_u), \quad h_i = \exp_{\circ}(z_i) \quad (9)$$

Hyperbolic Prediction Function. Through hyperbolic messaging passing, we've captured high-order relational information into hyperbolic embeddings. Hyperbolic distance is

now used to define a prediction function, which predicts the possibility that a user would interact with an item:

$$p(u, i) = \frac{1}{d_{\mathcal{H}}(h_u, h_i)} \quad (10)$$

Hyperbolic Margin Ranking and Informative Mechanism. To address the limitations of Euclidean-based approaches, we adopt the hyperbolic margin ranking loss (Sun et al., 2021), an extension of Bayesian Personalized Ranking (BPR) (Rendle et al., 2012). This loss pulls user-item pairs with observed interactions closer while pushing negative pairs apart, preventing the collapse seen in Euclidean space by incorporating a margin:

$$\ell_m(u, i, j) = \max(d_{\mathcal{H}}^2(h_u, h_i) - d_{\mathcal{H}}^2(h_u, h_j) + m, 0) \quad (11)$$

where $d_{\mathcal{H}}$ represents hyperbolic distance, m is the margin, (u, i) is an observed interaction, and (u, j) is a sampled negative pair.

To further refine this pull-push process, we integrate a geometric-aware mechanism (Yang et al., 2022a) combining Hyperbolic-aware Margin Learning (HAML) and Hyperbolic Informative Negative Sampling (HINS). HAML dynamically adjusts the margin based on hyperbolic geometry, assigning a larger margin to pairs near the origin:

$$\begin{aligned} m_{u,i}^{\mathcal{H}} &= \text{sigmoid}(\delta) \\ \delta &= \frac{d_{\mathcal{H}}^2(e_u, \mathbf{o}) + d_{\mathcal{H}}^2(e_i, \mathbf{o}) - d_{\mathcal{H}}^2(e_u, e_i)}{e_{u,0} \cdot e_{i,0}} \end{aligned} \quad (12)$$

where $e_{u,0}$ and $e_{i,0}$ are the zeroth coordinate elements of e_u and e_i , respectively, corresponding to the embeddings norms in the hyperbolic space. HINS enhances negative sampling by prioritizing candidates close to the positive

item, iteratively identifying the most informative negative samples. This method leverages hyperbolic geometry to effectively model head and tail items, improving utility performance in recommendations.

4.2. Semantic Representations Generation

In this subsection, we introduce a paradigm for distilling useful information from raw text descriptions of items and users into dense semantic embeddings, which will be used in our alignment framework to derive the final representation. Inspired by prior research (Ma et al., 2024; Ren et al., 2024) that leverages the power of large language models (LLMs) to extract useful user/item descriptions from raw, noisy textual data, we adopt a similar framework to generate user/item profiles with rich textual descriptions: $\mathcal{P}_i = LLMs(\mathcal{S}_i, \mathcal{T}_i)$, where \mathcal{S}_i represents system prompts to the LLMs, \mathcal{T}_i denotes raw textual information, and \mathcal{P}_i is the resulting user/item profile, consisting of sentence-level descriptions.

While we’ve derived textual information for users/items, it cannot be directly fused with the embeddings generated from hyperbolic collaborative filtering due to discrepancies in embedding geometry. To integrate both types of knowledge, we encode the textual information in embeddings using pre-trained text encoder models: $e_i = Encoder(\mathcal{P}_i)$. While LLM embeddings could be an alternative, they often introduce higher computational overhead and may not be optimized for alignment with hyperbolic representations, making encoders a more practical choice.

4.3. Hyperbolic Alignment

We propose maximizing mutual information between hyperbolic embeddings (collaborative information) and semantic embeddings (textual information) to create unified embeddings that integrate both knowledge types. To achieve this, we introduce a hyperbolic alignment loss, which reduces noise in representations and improves tail item recommendations by aligning information in the same hyperbolic space. A theoretical advantage of hyperbolic alignment over Euclidean alignment is discussed in the next subsection.

Before calculating the alignment loss, two steps are necessary: 1) the semantic embeddings must be adjusted to match the dimensionality of the collaborative embeddings, and 2) they should be transformed into a common representation space. To accomplish this, we first apply a multi-layer perceptron (MLP) to the semantic embeddings to ensure dimensional alignment. We then project the semantic embeddings into hyperbolic space so they can align with the hyperbolic collaborative embeddings:

$$s_i = \exp_x(e_i), \quad s'_i = MLP(s_i) \quad (13)$$

where \exp_x is defined as in Equation 3, e_i represents the semantic embeddings from the encoder, s_i is the dimension-

aligned semantic embedding, and s'_i denotes the final projected semantic embedding in hyperbolic space. The hyperbolic alignment loss is then calculated as:

$$\ell_{align}(i) = d_{\mathcal{H}}^2(h_i, s'_i) \quad (14)$$

where $d_{\mathcal{H}}$ represents the hyperbolic distance, and h_i is the hyperbolic embedding with collaborative information.

4.4. Gradient Analysis of Hyperbolic Alignment

To further explore the impact of aligning semantic embeddings within the hyperbolic model, we analyze the gradient behavior with respect to nodes of varying norms in Proposition 4.1, proof can be found in Appendix A. This provides insight into the hierarchical preservation properties of the hyperbolic space, which are absent in Euclidean space.

Proposition 4.1. *Let \mathbf{x}, \mathbf{y} denote embeddings in hyperbolic space \mathcal{H}^n with corresponding unit direction vectors in space-like dimension $\hat{\mathbf{x}}, \hat{\mathbf{y}}$, and let θ be the angle between them. The gradient magnitude of semantic alignment satisfies:*

$$\|\nabla_{\mathbf{x}} d_{\mathcal{H}}(\mathbf{x}, \mathbf{y})\| \approx \frac{\|\hat{\mathbf{x}} - \hat{\mathbf{y}}\|}{\|\mathbf{x}\|(1 - \cos \theta)}. \quad (15)$$

This facilitates adaptive gradient updates that intrinsically preserve hierarchical structures. In contrast, Euclidean space exhibits constant gradient magnitude $\|\nabla_{\mathbf{x}} d_{\mathcal{E}}(\mathbf{x}, \mathbf{y})\| = 1$, where $d_{\mathcal{H}}$ and $d_{\mathcal{E}}$ denote hyperbolic and Euclidean distances respectively.

This proposition highlights that hyperbolic space offers adaptive gradient magnitudes based on node norms. Nodes with large norms (fine-grained preferences, small positional changes cause significant distance changes) receive smaller gradient updates, ensuring precise distance adjustments and preserving local structures. Meanwhile, nodes with smaller norms (abstract preferences, positional changes have less impact on distances) adjust more, refining global relationships and effectively capturing the hierarchical structure.

4.5. Hierarchical Representation Structure

In this subsection, we design a mechanism that allows users to balance the exploration-exploitation trade-off by constructing a hierarchical representation structure based on the learned hyperbolic embeddings.

Hierarchy Tree. The primary motivation for constructing a hierarchy tree is to uncover hidden structures in the data that are not explicitly reflected in the dataset. For instance, consider the Amazon-CD dataset: a CD might be categorized under genres like “folk music”, but it cannot be labeled as “folk music preferred by teenagers”. However, in reality, such nuanced preferences exist within the collaborative

Algorithm 1 Hyperbolic Hierarchical Clustering

Input: Hyperbolic embeddings X , layer proportion k
Set the maximum number of layers $L = \log_k(|X|)$
Initialize the points of bottom layer $D_L = X$
for $l = L$ **to** 1 (bottom to top) **do**
 Randomly initialize cluster centroids in the hyperbolic space $M_l = \{\mu_l \mid \mu_l \in \mathbb{H}\}$, $|M_l| = |D_l|/k$
 repeat
 for each point $d_{l,i} \in D_l$ **do**
 Assign d_i to the cluster with the nearest centroid:
 $c_{l,i} = \arg \min_{\mu \in M_l} d_{\mathcal{H}}(d_i, \mu)$
 end for
 for each cluster $c_{l,i} \in C_l$ **do**
 Update the centroid $\mu_{l,i}$ as the hyperbolic mean $m_{\mathcal{H}}$ of all points assigned to cluster $c_{l,i}$:
 $\mu_{l,i} = m_{\mathcal{H}}(\{d \mid d \in C_{l,i}\})$
 end for
 until Centroids M_l do not change (convergence)
 Initialize the points of the upper layer $D_{l-1} = M_l$
end for

information. When recommending based solely on past interactions, we may overlook these hidden layers of structure that are implicit in the dataset (e.g., “music” \rightarrow “folk music” \rightarrow “folk music preferred by teenagers”).

To address this, we introduce a hyperbolic hierarchical clustering method based on hyperbolic embeddings to build the hierarchy tree. Specifically, we iteratively group embeddings into clusters and use the centroid of each cluster as the data point to be clustered in the upper layer, referred to as a pseudo-cluster node. However, the number of cluster nodes in each layer is not predefined and must be determined. Inspired by Dasgupta’s cost (Dasgupta, 2016), which encourages pushing edge cuts as far down the tree as possible, the optimal tree is required to be binary. Therefore, we fix the proportion of cluster nodes between layers as $k = 2$. The details of the algorithm are presented in Algorithm 1.

Exploration-Exploitation Balance. To allow users to balance the exploration-exploitation trade-off, we introduce two adjustable parameters: temperature τ and hierarchy layer l . In the standard recommendation approach, items are recommended based on similarity to the user’s embedding, which may limit exploration. For users with focused preferences, this method may consistently recommend items that align too closely with their past choices, offering little opportunity to explore different categories.

To address this issue, we modify the recommendation process by replacing a portion of the recommended items with alternatives from other branches in the hierarchy tree. This modification gives users control over the balance between exploration and exploitation. Temperature τ allows users

to specify the proportion of original recommendations to replace, while layer l determines the starting point for exploration. For example, suppose a user selects $\tau = 0.5$ and $l = 5$. In that case, half of the original recommendations are retained, and the other half is replaced with items sampled from its ancestor cluster at layer 5 of the hierarchy tree.

Complexity Analysis. To demonstrate the scalability and efficiency of our approach, we analyze the complexity of constructing and applying the hierarchical representation structure. Let N denote the total number of users and items, and let k be the number of recommendations per user. The hierarchy tree is built using iterative k -means clustering in hyperbolic space, where cluster nodes are assigned only to real node embeddings for efficiency.

First, computing and storing pairwise distances requires $O(N^2/2)$ operations. Each k -means iteration has complexity $O(i)$, and with $O(\log N)$ hierarchical levels, the total complexity of constructing the hierarchy tree is: $O\left(\frac{N^2}{2} + i \log N\right)$. For recommendation retrieval, finding the top- k recommendations involves nearest neighbor search in hyperbolic space, which runs in $O(k \log N)$. Adjusting recommendations by retrieving ancestor clusters at layer l requires only tree traversal, which runs in $O(k)$.

Overall, our hierarchical framework ensures efficient scaling while maintaining flexibility in recommendation adjustments. This design enables HERec to dynamically balance exploration and exploitation while ensuring scalability for large-scale recommender systems.

5. EXPERIMENTS

5.1. Experimental Settings

Datasets. To evaluate our proposed model, we utilize three widely-used public datasets: **Amazon-books**, which contains user purchase behaviors within the book category on Amazon; **Yelp**, which records customer ratings and reviews for restaurants on Yelp; and **Google-reviews**, which includes user reviews and business metadata from Google Maps. Detailed statistics, including the distribution of head and tail items, are provided in Table 3. The high proportion of tail users (T80) highlights the prevalence of long-tail distributions, supporting the assumption of a power-law distribution in real-world data.

Evaluation Metrics. We assess our recommended items using both utility and diversity metrics, demonstrating that our model achieves precise recommendations for users’ preference while enhancing diversity in the recommendation. For utility, we adopt two widely used ranking metrics: Recall and NDCG, which measure the effectiveness of the model. To evaluate diversity, we employ three metrics: Distance Diversity (Div) (Ziegler et al., 2005; Zhang & Hurley, 2008),

Title Suppressed Due to Excessive Size

Table 1. Comprehensive model comparison based on utility and diversity metrics, where higher values signify superior performance. The best-performing results for each metric are highlighted in bold, with the second-best results underlined.

Data	Models	Utility \uparrow				Diversity \uparrow					
		Recall@10	NDCG@10	Recall@20	NDCG@20	Div@10	H@10	EPC@10	Div@20	H@20	EPC@20
Amazon-books	LightGCN	0.0950	0.0726	0.1428	0.0884	0.4469	9.8554	0.7429	0.4504	10.485	0.7798
	TAG-CF	0.0986	0.0755	0.1468	0.0912	0.4090	10.915	0.7899	0.4517	11.465	0.8227
	LightGCL	0.1075	0.0846	0.1515	0.0991	0.4651	11.511	0.8523	0.4974	11.941	0.8728
	SimGCL	0.0997	0.0762	0.1478	0.0918	0.4286	10.341	0.7757	0.4802	10.915	0.8076
	HCCF	0.1045	0.0813	0.1488	0.0962	<u>0.5008</u>	11.814	0.8579	<u>0.5433</u>	<u>12.137</u>	<u>0.8746</u>
	HGCF	0.1013	0.0759	0.1511	0.0921	0.4742	11.577	<u>0.8623</u>	0.5041	11.732	0.8585
	HICF	0.1113	<u>0.0862</u>	<u>0.1599</u>	<u>0.1022</u>	0.4702	<u>11.922</u>	0.8561	0.5261	12.129	0.8660
	Ours	0.1167	0.0902	0.1682	0.1069	0.5255	12.096	0.8700	0.5754	12.254	0.8758
	Yelp	LightGCN	0.0678	0.0565	0.1135	0.0717	0.2603	8.3263	0.6842	0.2277	9.1811
TAG-CF		0.0692	0.0571	0.1142	0.0722	0.2353	8.4516	0.6939	0.2276	9.3108	0.7428
LightGCL		<u>0.0709</u>	<u>0.0594</u>	0.1141	0.0739	0.2856	11.243	0.8281	0.3064	11.823	0.8550
SimGCL		0.0707	0.0586	<u>0.1184</u>	<u>0.0748</u>	0.3397	9.8191	0.7642	0.3460	10.508	0.7973
HCCF		0.0680	0.0562	0.1097	0.0701	0.3168	11.942	0.8572	0.3535	<u>12.311</u>	<u>0.8752</u>
HGCF		0.0654	0.0510	0.1099	0.0665	0.3133	<u>11.977</u>	0.8718	0.3289	12.103	0.8747
HICF		<u>0.0709</u>	0.0579	0.1169	0.0737	<u>0.3478</u>	<u>11.877</u>	0.8557	<u>0.3721</u>	12.147	0.8666
Ours		0.0739	0.0597	0.1224	0.0762	0.3874	12.155	<u>0.8716</u>	0.3961	12.329	0.8773
Google-reviews		LightGCN	0.0932	0.0745	0.1430	0.0929	0.2422	9.9149	0.7241	0.2725	10.761
	TAG-CF	0.0942	0.0754	0.1447	0.0940	0.2376	10.184	0.7485	0.2497	11.031	0.7961
	LightGCL	0.0945	0.0768	0.1461	0.0959	0.2639	11.643	0.8333	0.2705	12.317	<u>0.8655</u>
	SimGCL	<u>0.0979</u>	0.0784	0.1482	<u>0.0971</u>	0.2966	10.361	0.7486	0.2950	11.119	0.7923
	HCCF	0.0923	0.0744	0.1446	0.0937	0.2195	10.741	0.8056	0.2402	11.561	0.8433
	HGCF	0.0910	0.0697	0.1485	0.0909	0.2859	12.248	<u>0.8538</u>	0.3321	12.474	0.8619
	HICF	0.0951	0.0736	<u>0.1515</u>	0.0944	0.3262	<u>12.376</u>	0.8523	<u>0.3510</u>	<u>12.660</u>	0.8640
	Ours	0.1002	<u>0.0772</u>	0.1598	0.0992	<u>0.3185</u>	12.466	0.8598	0.3543	12.769	0.8728

Table 2. Comparison with feature-enhanced Euclidean baselines, with the best-performing results highlighted in bold.

Data	Amazon-books					Yelp					Google-reviews				
Metrics	R@20	N@20	Div@20	H@20	EPC@20	R@20	N@20	Div@20	H@20	EPC@20	R@20	N@20	Div@20	H@20	EPC@20
LightGCN+	0.1466	0.0901	0.4349	10.3915	0.7802	0.1156	0.0733	0.2697	9.6903	0.7526	0.1438	0.0940	0.2707	10.8664	0.7801
LightGCL+	0.1545	0.0992	0.5064	11.9761	0.8728	0.1131	0.0739	0.2759	11.8617	0.8581	0.1443	0.0946	0.2744	12.4700	0.8776
SimGCL+	0.1494	0.0926	0.5163	11.4751	0.8342	0.1195	0.0752	0.3152	9.9952	0.7811	0.1504	0.0982	0.3030	11.2111	0.7953
HCCF+	0.1525	0.0940	0.4316	11.7984	0.8616	0.1170	0.0729	0.2884	11.6906	0.8577	0.1438	0.0941	0.2524	11.5433	0.8406
Ours	0.1682	0.1069	0.5754	12.2543	0.8758	0.1224	0.0762	0.3961	12.3290	0.8773	0.1598	0.0992	0.3543	12.7690	0.8728

Table 3. Statistics of the experimental data.

Dataset	#User	#Item			#Interactions	Density
		All	H20(%)	T80(%)		
Amazon-books	11,000	9,332	45.2	54.8	120,464	1.17e ⁻³
Yelp	11,091	11,010	47.0	53.0	166,620	1.36e ⁻³
Google-reviews	22,582	16,557	46.8	53.2	411,840	1.10e ⁻³

Shannon Entropy (H) (Mehta et al., 2012), and Expected Popularity Complement (EPC) (Vargas & Castells, 2011).

Distance Diversity (Div) quantifies the variation among recommended items, encouraging diversity within the recommendation:

$$Div(u) = \frac{\sum_{i \in R_u} \sum_{j \in R_u, j \neq i} d(i, j)}{\text{Number of } (i, j) \text{ pairs}} \quad (16)$$

where R_u is the recommendation list for user u , and $d(i, j)$ represents the distance between items i and j . Number of (i, j) pairs is calculated as $\binom{|R_u|}{2} = \frac{|R_u|(|R_u|-1)}{2}$. For fair comparison, we compute distances within the same representation space across models.

Shannon Entropy (H) quantifies the unpredictability within the recommendations, with higher entropy signifying greater diversity:

$$H = - \sum_{i \in \text{set}(\sum_u R_u)} p(i) \log p(i) \quad (17)$$

where $\sum_u R_u$ denotes all recommended items across users (including duplicates), and $p(i) = \text{count}(i) / \sum_{i \in \text{set}(\sum_u R_u)} \text{count}(i)$ is the proportion of item i among all recommended items.

Expected Popularity Complement (EPC) assesses the extent of bias towards popular items by promoting niche recommendations:

$$EPC = 1 - \frac{1}{|\text{set}(\sum R_u)|} \sum_{i \in \text{set}(\sum_u R_u)} \frac{\text{pop}(i)}{\max_i(\text{pop}(i))} \quad (18)$$

where N_u is the set of items user u has interacted with, and $\text{pop}(i) = \text{count}(i) / \sum_{i \in \text{set}(\sum_u N_u)} \text{count}(i)$ denotes item i 's popularity.

Baselines. We compare our model with state-of-the-art baselines in both Euclidean and Hyperbolic spaces:

- **LightGCN** (He et al., 2020): A lightweight graph convolution neural network model for recommendation by removing redundant neural modules in graph convolution.
- **TAG-CF** (Ju et al., 2024): A test-time augmentation framework that enhances recommendation by performing a single message-passing step only at inference time.
- **LightGCL** (Cai et al., 2023): A contrastive learning model that uses singular value decomposition (SVD) for robust graph augmentation without data augmentation.

Table 4. Performance on H20 (head) and T80 (tail) items, with the top hyperbolic results highlighted in bold. $\Delta_{\mathcal{H}}(\%)$ represents the improvement over the second-best hyperbolic baseline, which is underlined.

Datasets	Amazon-books				Yelp				Google-reviews			
	Recall@20		NDCG@20		Recall@20		NDCG@20		Recall@20		NDCG@20	
	H20	T80	H20	T80	H20	T80	H20	T80	H20	T80	H20	T80
LightGCN	0.1162	0.0266	0.0744	0.0140	0.1076	0.0059	0.0693	0.0024	0.1311	0.0119	0.0878	0.0051
HGCF	0.1083	0.0428	0.0673	0.0248	0.0789	0.0310	0.0489	0.0176	0.1123	0.0362	0.0714	0.0195
HICF	0.1086	0.0513	0.0713	0.0309	0.0847	0.0322	0.0556	0.0180	0.1147	0.0388	0.0746	0.0208
Ours	0.1125	0.0557	0.0730	0.0339	0.0863	0.0361	0.0558	0.0204	0.1155	0.0443	0.0755	0.0238
$\Delta_{\mathcal{H}}(\%)$	+3.59	+8.58	+2.38	+9.71	+1.89	+12.11	+0.36	+13.33	+0.70	+14.18	+1.21	+14.42

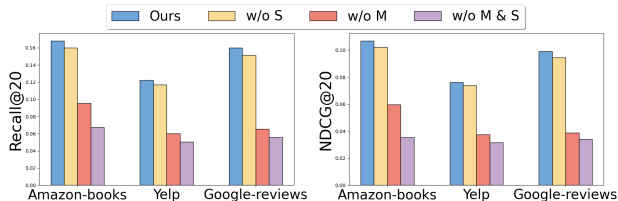


Figure 3. Ablation study on model variants.

- **SimGCL** (Yu et al., 2022): A contrastive learning model that replaces graph augmentations in contrastive learning by introducing random noise during initialization.
- **HCCF** (Xia et al., 2022): A collaborative filtering framework that integrates hypergraph and contrastive learning, capturing both local and global user dependencies.
- **HGCF** (Sun et al., 2021): A hyperbolic GNN model that combines hypergraph learning with collaborative filtering using hyperbolic margin ranking loss.
- **HICF** (Yang et al., 2022a): A hyperbolic recommendation model that enhances head and tail item performance with hyperbolic geometry, improving utility for long-tail items.

Training Details. We set embedding dimensions to 50 and a training batch size of 1024. Embeddings in hyperbolic space are optimized using Riemannian SGD (RSGD) (Bécigneul & Ganea, 2018; Sun et al., 2021), while the MLP adapter is optimized with Adam (Kingma, 2014). Training incorporates early stopping technique based on Recall@10 with 10 patience steps. We generate user and item profiles using GPT-3.5-turbo and encode them with text-embedding-ada-002 (Neelakantan et al., 2022) for Amazon-books and Yelp, and BERT (Devlin, 2018) for Google-reviews. All experiments are conducted on NVIDIA A40/A100 GPUs with 40GB memory.

5.2. Performance Comparison

Overall Comparison. The performance comparison across all models is presented in Table 1. Our HERec consistently outperforms the baselines in both utility and diversity metrics, achieving up to 5.49% improvement in utility metrics and 11.39% increase in diversity metrics. Notably, most baselines struggle to achieve strong performance in both utility and diversity simultaneously. For instance, while HICF performs second-best in utility metrics on the Amazon-books dataset, it lacks the same advantage in diver-

sity metrics, where several baselines achieve better results. This highlights the superiority of our model, which achieves state-of-the-art performance in both utility and diversity: a feat not previously attained by any baseline.

Baselines with Feature Enhancement. To ensure a fair comparison, we further enhance Euclidean baselines by integrating feature information. Specifically, we align semantic embeddings with the original Euclidean embeddings following the structure in Section 4.2, but in Euclidean space. The results are presented in Table 2, with enhanced baselines denoted by “+”. The data shows that our HERec still surpasses all baselines in both utility and diversity. Interestingly, while the feature-enhanced versions of the Euclidean baselines generally improve in utility metrics, they do not exhibit a stable improvement in diversity metrics. This aligns with our theoretical analysis in Section 4.4, which demonstrates the advantages of our alignment in the hyperbolic space.

Additionally, to validate the effectiveness of our alignment framework in capturing semantics, we designed a profile decoder module to reconstruct user and item profiles from the learned hyperbolic embeddings. The results demonstrate that profiles reconstructed from our model’s embeddings exhibit higher alignment with the originals, confirming the model’s ability to effectively capture underlying semantic meaning. Detailed methodology and experimental results are provided in Appendix B.

Performance on Head and Tail Items. To underscore the effectiveness of semantic alignment, particularly for cold-start (tail) items, we conducted experiments measuring utility performance on both head and tail items. In our context, head items (H20) refer to the top 20% of items with the highest number of interactions in the training dataset, representing the most popular items. The remaining items are categorized as tail items (T80), which have limited interaction history, representing less frequently engaged items.

For simplicity, we compare our model with all hyperbolic baselines and a representative Euclidean baseline (LightGCN). The results, displayed in Table 4, reveal significant improvements, especially for tail items. Compared with hyperbolic baselines without semantic alignment, our model shows a notably larger performance boost on tail items than on head items. This finding indicates that semantic alignment particularly enhances the recommendation of cold-start items, effectively mitigating the cold-start problem for

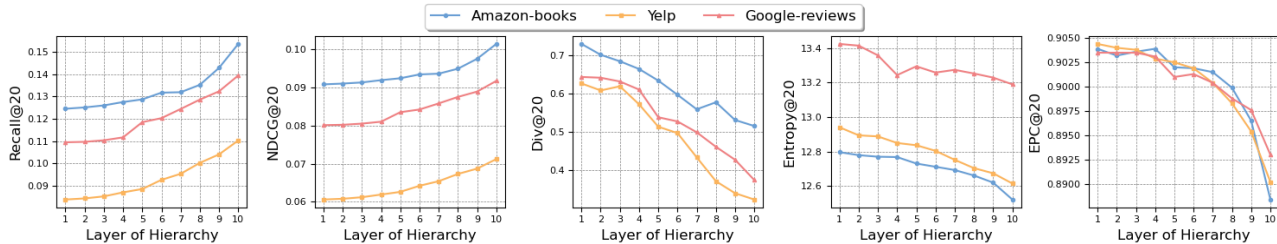


Figure 4. Performance analysis across hierarchical structure layers.

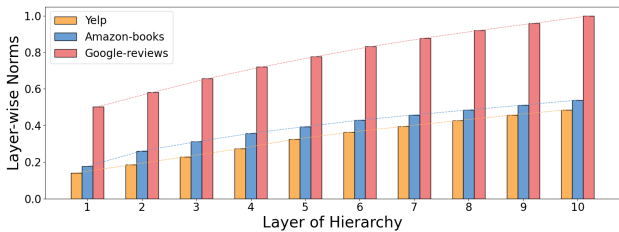


Figure 5. Layer-wise norms within the hierarchy structure.

items with limited or no prior interactions.

5.3. Ablation Study

We perform an ablation study to examine the contributions of two key components in our model: hyperbolic margin ranking loss and semantic alignment loss. To maintain meaningful evaluation, we focus solely on utility metrics, as random recommendations may artificially inflate diversity without practical utility. The following notations are used for our ablation variants: “w/o M” denotes the model without hyperbolic margin ranking loss, “w/o S” represents the model without semantic alignment loss, and “w/o M & S” indicates that both margin ranking and semantic alignment are excluded, leaving only the BPR loss.

Figure 3 shows that our full model outperforms all ablation variants, highlighting its overall effectiveness. Models lacking both margin ranking and semantic alignment perform the worst, while removing either module results in decreased utility, emphasizing the effectiveness of integration.

5.4. Hierarchical Representation Structure Analysis

We evaluated the effectiveness of our hierarchical representation structure through experiments simulating varying user preferences. Using a temperature parameter $\tau = 0.5$ to control recommendation randomness, we analyzed performance across various hierarchical layers. As shown in Figure 4, utility metrics increase while diversity metrics decrease with larger layers. This trade-off aligns with the model’s design: larger layers focus on utility and specific interests for exploitation, while smaller layers prioritize diversity for exploration. This structure provides users with a flexible mechanism to adjust recommendations from niche,

relevant items to broader, exploratory sets based on their preferences. A case study is provided in Appendix C.

Additionally, to validate the hierarchical structure’s capability to capture varying degrees of group preferences, we analyzed the average norm of node embeddings across layers (Figure 5). The results reveal a consistent increase at larger layers (farther from the center in hyperbolic space). As previously mentioned, hyperbolic geometry ensures that popular items or exploratory users are positioned closer to the origin, while niche items or users are positioned toward the boundaries. This finding aligns seamlessly with the properties of hyperbolic space, validating the intended design of the hierarchical structure: higher-level (smaller-layer) nodes effectively encapsulate abstract and aggregated preferences, whereas lower-level (larger-layer) nodes focus on fine-grained, personalized preferences.

6. CONCLUSION

In this work, we present HERec, a hyperbolic graph-LLM framework that effectively balances exploration and exploitation in recommender systems. Our approach integrates semantic and collaborative information within hyperbolic space, leveraging the unique properties of hyperbolic geometry. Furthermore, we introduce a personalized mechanism for balancing the exploration-exploitation trade-off using a hierarchical representation structure, empowering users to adjust recommendation preferences flexibly. Extensive experiments demonstrate that our model achieves state-of-the-art performance, achieving up to a 5.49% improvement in utility metrics and an 11.39% increase in diversity metrics. Remarkably, HERec is the first framework to excel in both utility and diversity simultaneously, marking a significant advancement in the field.

ACKNOWLEDGEMENTS

This work was partially supported by the National Science Foundation (NSF) IIS Div Of Information & Intelligent Systems 2403317. We also gratefully acknowledge partial support from an Amazon Research Award, funding generously provided by Snap Research, and resources made available by the Yale Office of the Provost.

Impact Statement

This paper presents work whose goal is to advance the field of Machine Learning. There are many potential societal consequences of our work, none which we feel must be specifically highlighted here.

References

- Bao, K., Zhang, J., Zhang, Y., Wang, W., Feng, F., and He, X. Tallrec: An effective and efficient tuning framework to align large language model with recommendation. In *Proceedings of the 17th ACM Conference on Recommender Systems*, pp. 1007–1014, 2023.
- Bécigneul, G. and Ganea, O.-E. Riemannian adaptive optimization methods. *arXiv preprint arXiv:1810.00760*, 2018.
- Cai, X., Huang, C., Xia, L., and Ren, X. Lightgcl: Simple yet effective graph contrastive learning for recommendation. *arXiv preprint arXiv:2302.08191*, 2023.
- Castells, P., Hurley, N., and Vargas, S. Novelty and diversity in recommender systems. In *Recommender systems handbook*, pp. 603–646. Springer, 2021.
- Chami, I., Ying, Z., Ré, C., and Leskovec, J. Hyperbolic graph convolutional neural networks. *Advances in neural information processing systems*, 32, 2019.
- Chen, H., Shi, S., Li, Y., and Zhang, Y. Neural collaborative reasoning. In *Proceedings of the Web Conference 2021*, pp. 1516–1527, 2021.
- Dasgupta, S. A cost function for similarity-based hierarchical clustering. In *Proceedings of the forty-eighth annual ACM symposium on Theory of Computing*, pp. 118–127, 2016.
- Devlin, J. Bert: Pre-training of deep bidirectional transformers for language understanding. *arXiv preprint arXiv:1810.04805*, 2018.
- Du, Y., Zhu, X., Chen, L., Zheng, B., and Gao, Y. Hakg: Hierarchy-aware knowledge gated network for recommendation. In *Proceedings of the 45th international ACM SIGIR conference on Research and development in Information Retrieval*, pp. 1390–1400, 2022.
- Ganea, O., Bécigneul, G., and Hofmann, T. Hyperbolic neural networks. *Advances in neural information processing systems*, 31, 2018.
- He, X., Deng, K., Wang, X., Li, Y., Zhang, Y., and Wang, M. Lightgcn: Simplifying and powering graph convolution network for recommendation. In *Proceedings of the 43rd International ACM SIGIR conference on research and development in Information Retrieval*, pp. 639–648, 2020.
- Ju, M., Shiao, W., Guo, Z., Ye, Y., Liu, Y., Shah, N., and Zhao, T. How does message passing improve collaborative filtering? *arXiv preprint arXiv:2404.08660*, 2024.
- Kingma, D. P. Adam: A method for stochastic optimization. *arXiv preprint arXiv:1412.6980*, 2014.
- Koren, Y., Bell, R., and Volinsky, C. Matrix factorization techniques for recommender systems. *Computer*, 42(8): 30–37, 2009.
- Krioukov, D., Papadopoulos, F., Kitsak, M., Vahdat, A., and Boguná, M. Hyperbolic geometry of complex networks. *Physical Review E—Statistical, Nonlinear, and Soft Matter Physics*, 82(3):036106, 2010.
- Kunaver, M. and Požrl, T. Diversity in recommender systems—a survey. *Knowledge-based systems*, 123:154–162, 2017.
- Li, J., Wang, M., Li, J., Fu, J., Shen, X., Shang, J., and McAuley, J. Text is all you need: Learning language representations for sequential recommendation. In *Proceedings of the 29th ACM SIGKDD Conference on Knowledge Discovery and Data Mining*, pp. 1258–1267, 2023.
- Liu, Q., Nickel, M., and Kiela, D. Hyperbolic graph neural networks. *Advances in neural information processing systems*, 32, 2019.
- Lyu, H., Jiang, S., Zeng, H., Xia, Y., Wang, Q., Zhang, S., Chen, R., Leung, C., Tang, J., and Luo, J. Llm-rec: Personalized recommendation via prompting large language models. *arXiv preprint arXiv:2307.15780*, 2023.
- Ma, Q., Ren, X., and Huang, C. Xrec: Large language models for explainable recommendation. *arXiv preprint arXiv:2406.02377*, 2024.
- Mehta, H., Bhatia, S. K., Bedi, P., and Dixit, V. S. Collaborative personalized web recommender system using entropy based similarity measure. *arXiv preprint arXiv:1201.4210*, 2012.
- Neelakantan, A., Xu, T., Puri, R., Radford, A., Han, J. M., Tworek, J., Yuan, Q., Tezak, N., Kim, J. W., Hallacy, C., et al. Text and code embeddings by contrastive pre-training. *arXiv preprint arXiv:2201.10005*, 2022.
- Ren, X., Wei, W., Xia, L., Su, L., Cheng, S., Wang, J., Yin, D., and Huang, C. Representation learning with large language models for recommendation. In *Proceedings of the ACM on Web Conference 2024*, pp. 3464–3475, 2024.
- Rendle, S., Freudenthaler, C., Gantner, Z., and Schmidt-Thieme, L. Bpr: Bayesian personalized ranking from implicit feedback. *arXiv preprint arXiv:1205.2618*, 2012.

- Sun, J., Cheng, Z., Zuberi, S., Pérez, F., and Volkovs, M. Hgcf: Hyperbolic graph convolution networks for collaborative filtering. In *Proceedings of the Web Conference 2021*, pp. 593–601, 2021.
- Tai, C.-Y., Huang, C.-K., Huang, L.-Y., and Ku, L.-W. Knowledge based hyperbolic propagation. In *Proceedings of the 44th International ACM SIGIR Conference on Research and Development in Information Retrieval*, pp. 1945–1949, 2021.
- Unger, M. and Tuzhilin, A. Hierarchical latent context representation for context-aware recommendations. *IEEE Transactions on Knowledge and Data Engineering*, 34(7):3322–3334, 2020.
- Vargas, S. and Castells, P. Rank and relevance in novelty and diversity metrics for recommender systems. In *Proceedings of the fifth ACM conference on Recommender systems*, pp. 109–116, 2011.
- Vinh Tran, L., Tay, Y., Zhang, S., Cong, G., and Li, X. Hyperml: A boosting metric learning approach in hyperbolic space for recommender systems. In *Proceedings of the 13th international conference on web search and data mining*, pp. 609–617, 2020.
- Wang, X., He, X., Wang, M., Feng, F., and Chua, T.-S. Neural graph collaborative filtering. In *Proceedings of the 42nd international ACM SIGIR conference on Research and development in Information Retrieval*, pp. 165–174, 2019.
- Wei, W., Ren, X., Tang, J., Wang, Q., Su, L., Cheng, S., Wang, J., Yin, D., and Huang, C. Llmrec: Large language models with graph augmentation for recommendation. In *Proceedings of the 17th ACM International Conference on Web Search and Data Mining*, pp. 806–815, 2024.
- Wilson, R. C., Bonawitz, E., Costa, V. D., and Ebitz, R. B. Balancing exploration and exploitation with information and randomization. *Current opinion in behavioral sciences*, 38:49–56, 2021.
- Wu, J., Wang, X., Feng, F., He, X., Chen, L., Lian, J., and Xie, X. Self-supervised graph learning for recommendation. In *Proceedings of the 44th international ACM SIGIR conference on research and development in information retrieval*, pp. 726–735, 2021.
- Xi, Y., Liu, W., Lin, J., Cai, X., Zhu, H., Zhu, J., Chen, B., Tang, R., Zhang, W., and Yu, Y. Towards open-world recommendation with knowledge augmentation from large language models. In *Proceedings of the 18th ACM Conference on Recommender Systems*, pp. 12–22, 2024.
- Xia, L., Huang, C., Xu, Y., Zhao, J., Yin, D., and Huang, J. Hypergraph contrastive collaborative filtering. In *Proceedings of the 45th International ACM SIGIR conference on research and development in information retrieval*, pp. 70–79, 2022.
- Yang, M., Li, Z., Zhou, M., Liu, J., and King, I. Hicf: Hyperbolic informative collaborative filtering. In *Proceedings of the 28th ACM SIGKDD Conference on Knowledge Discovery and Data Mining*, pp. 2212–2221, 2022a.
- Yang, M., Zhou, M., Liu, J., Lian, D., and King, I. Hrcf: Enhancing collaborative filtering via hyperbolic geometric regularization. In *Proceedings of the ACM Web Conference 2022*, pp. 2462–2471, 2022b.
- Yang, M., Zhou, M., Pan, L., and King, I. κ hgcn: Tree-likeness modeling via continuous and discrete curvature learning. In *Proceedings of the 29th ACM SIGKDD Conference on Knowledge Discovery and Data Mining*, pp. 2965–2977, 2023.
- Ying, R., He, R., Chen, K., Eksombatchai, P., Hamilton, W. L., and Leskovec, J. Graph convolutional neural networks for web-scale recommender systems. In *Proceedings of the 24th ACM SIGKDD international conference on knowledge discovery & data mining*, pp. 974–983, 2018.
- Yu, J., Yin, H., Xia, X., Chen, T., Cui, L., and Nguyen, Q. V. H. Are graph augmentations necessary? simple graph contrastive learning for recommendation. In *Proceedings of the 45th international ACM SIGIR conference on research and development in information retrieval*, pp. 1294–1303, 2022.
- Zhang, M. and Hurley, N. Avoiding monotony: improving the diversity of recommendation lists. In *Proceedings of the 2008 ACM conference on Recommender systems*, pp. 123–130, 2008.
- Zhang, T., Kishore, V., Wu, F., Weinberger, K. Q., and Artzi, Y. Bertscore: Evaluating text generation with bert. *arXiv preprint arXiv:1904.09675*, 2019.
- Zhang, Y., Wang, X., Shi, C., Liu, N., and Song, G. Lorentzian graph convolutional networks. In *Proceedings of the web conference 2021*, pp. 1249–1261, 2021.
- Zhang, Y., Feng, F., Zhang, J., Bao, K., Wang, Q., and He, X. Collm: Integrating collaborative embeddings into large language models for recommendation. *arXiv preprint arXiv:2310.19488*, 2023.
- Zheng, B., Hou, Y., Lu, H., Chen, Y., Zhao, W. X., Chen, M., and Wen, J.-R. Adapting large language models by integrating collaborative semantics for recommendation. In *2024 IEEE 40th International Conference on Data Engineering (ICDE)*, pp. 1435–1448. IEEE, 2024.

Zheng, L., Cao, B., Noroozi, V., Philip, S. Y., and Ma, N. Hierarchical collaborative embedding for context-aware recommendations. In *2017 IEEE International Conference on Big Data (Big Data)*, pp. 867–876. IEEE, 2017.

Ziegler, C.-N., McNee, S. M., Konstan, J. A., and Lausen, G. Improving recommendation lists through topic diversification. In *Proceedings of the 14th international conference on World Wide Web*, pp. 22–32, 2005.

A. Proof

In this section, we provide a rigorous mathematical proof of Proposition 4.1, demonstrating the unique advantage of the aligning mechanism in the hyperbolic space.

A.1. Gradient Analysis in Hyperbolic Space.

Suppose \mathbf{x} is a hyperbolic embedding derived from 4.1, and \mathbf{y} is the corresponding semantic embedding from 4.2, the hyperbolic distance is given by:

$$d_{\mathcal{H}}(\mathbf{x}, \mathbf{y}) = \operatorname{arccosh}(z) \quad (19)$$

where $z = -\langle \mathbf{x}, \mathbf{y} \rangle_{\mathcal{L}} = x_0 y_0 - \sum_{i=1}^n x_i y_i$.

For large $\|\mathbf{x}\|$ and $\|\mathbf{y}\|$, given $x_0 = \sqrt{1 + \|\mathbf{x}\|^2}$ and $y_0 = \sqrt{1 + \|\mathbf{y}\|^2}$, we adopt the following approximations for further calculation:

$$x_0 \approx \|\mathbf{x}\|, \quad y_0 \approx \|\mathbf{y}\|, \quad \sqrt{z^2 - 1} \approx z \quad (20)$$

Thus, the Lorentz product can be approximated as:

$$z = x_0 y_0 - \sum_{i=1}^n x_i y_i \approx \|\mathbf{x}\| \|\mathbf{y}\| (1 - \cos \theta) \quad (21)$$

Let $x_j = \|\mathbf{x}\| \hat{x}_j$ and $y_j = \|\mathbf{y}\| \hat{y}_j$ (where \hat{x}_j represents the direction of x_j). The partial derivative of z with respect to x_j is calculated as follows:

$$\begin{aligned} \frac{\partial z}{\partial x_j} &= \frac{x_j}{x_0} y_0 - y_j \\ &\approx \frac{x_j}{\|\mathbf{x}\|} \|\mathbf{y}\| - y_j \\ &= \|\mathbf{y}\| (\hat{x}_j - \hat{y}_j) \end{aligned} \quad (22)$$

Therefore, the gradient norm of $d_{\mathcal{H}}$ for \mathbf{x} can be approximated by:

$$\begin{aligned} \|\nabla_{\mathbf{x}} d_{\mathcal{H}}\| &= \frac{\|\nabla_{\mathbf{x}} z\|}{\sqrt{z^2 - 1}} \\ &\approx \frac{\|\nabla_{\mathbf{x}} z\|}{z} \\ &= \frac{\|\mathbf{y}\| \|\hat{\mathbf{x}} - \hat{\mathbf{y}}\|}{\|\mathbf{x}\| \|\mathbf{y}\| (1 - \cos \theta)} \\ &= \frac{\|\hat{\mathbf{x}} - \hat{\mathbf{y}}\|}{\|\mathbf{x}\| (1 - \cos \theta)} \end{aligned} \quad (23)$$

System Instruction:

Describe what types of items this user is likely to enjoy/
Describe what types of users would enjoy this item.

Input Prompt:

<USER_EMBED>/<ITEM_EMBED>

Output:

The user would prefer items which .../
The item would be preferred by users who ...

Figure 6. A depiction of model prompt instruction.

This result suggests that nodes with large norms experience smaller gradient updates, preserving local structures, while nodes with smaller norms undergo larger updates, refining global hierarchical relationships and effectively capturing hierarchical structures. This aligns with the properties of hyperbolic geometry, where small positional changes near the origin result in significant distance changes, and vice versa. Our dynamic gradient update mechanism is well-suited to this characteristic, enabling precise adjustments and enhancing the accuracy of the updates.

A.2. Gradient Analysis Euclidean Space.

For comparison, we examine the gradient behavior in Euclidean space. The Euclidean distance is defined as:

$$f(\mathbf{x}) = d_E(\mathbf{x}, \mathbf{y}) = \|\mathbf{x} - \mathbf{y}\| \quad (24)$$

The gradient of $f(\mathbf{x})$ with respect to \mathbf{x} is:

$$\nabla_{\mathbf{x}} f(\mathbf{x}) = \frac{\mathbf{x} - \mathbf{y}}{\|\mathbf{x} - \mathbf{y}\|} = \frac{\mathbf{x} - \mathbf{y}}{d_E(\mathbf{x}, \mathbf{y})} \quad (25)$$

which has a magnitude of:

$$\|\nabla_{\mathbf{x}} f(\mathbf{x})\| = 1 \quad (26)$$

The constant gradient magnitude demonstrates Euclidean space’s uniform update behavior, lacking intrinsic adaptation to hierarchical structures. This fundamental difference in gradient dynamics explains hyperbolic space’s superiority for hierarchical representation learning.

B. Profile Decoder

To further evaluate the effectiveness of hyperbolic alignment and the expressiveness of our learned hyperbolic embeddings, we introduce a profile decoder designed to reconstruct the original profile from these embeddings, thereby broadening their application beyond recommendation tasks. Our method begins by mapping the hyperbolic embeddings back into Euclidean space to facilitate alignment with traditional network layers. These Euclidean-mapped embeddings are then processed through a mixture of experts (MoE) module. The MoE serves to refine the embeddings, ensuring

consistency in both dimensionality and semantic representation (Ma et al., 2024). Once processed, these embeddings are fed into the language model, specifically after the positional layer, to incorporate them within a sequential architecture. To enhance training efficiency and minimize computational cost, we freeze the language model’s parameters, making the MoE module the only trainable component in the architecture.

Details of the input prompt structure and processing flow are depicted in Figure 6. To facilitate seamless embedding integration, we introduce two additional tokens, $\langle USER_EMBED \rangle$ and $\langle ITEM_EMBED \rangle$, to the language model’s tokenizer. This addition enables these embeddings to be treated as single, coherent tokens, ensuring accurate tokenization. After passing through the positional layer, the placeholders are dynamically replaced by the adapted embeddings generated by the MoE, allowing the embeddings to retain context-specific information.

B.1. Decoder Quality

To assess the effectiveness of our decoder mechanism, we compare the embeddings from our model against those from Euclidean embeddings (LightGCN) and Hyperbolic embeddings (HICF) as inputs to the decoder. The results are shown in Table 5. We use BERTScore (Zhang et al., 2019) to evaluate the semantic alignment of generated sentences with the original profile. Results indicate that our HERec outperforms both Euclidean and hyperbolic baselines, demonstrating that our model’s embeddings support recommendation and retain user/item profile information. This finding underscores that our model captures collaborative information alongside recoverable language semantics: a capability not achieved by previous models.

B.2. Decoder Case Study

To vividly illustrate the semantic capacity of our embeddings, we present two case studies demonstrating the model’s ability to recover user and item profiles.

Original user profile:

Based on the user’s interactions and reviews, this user is likely to enjoy unique dining experiences with a variety of options, trendy atmosphere with good drink and food selections, premium quality frozen yogurt with a wide variety of toppings, creative burgers and hot dogs, delicious Thai cuisine, and authentic and spicy Chinese cuisine served family-style.

Recovered user profile:

Based on the user’s interactions, it is likely that they would enjoy businesses that offer a variety of cuisines, including Mexican, Italian, and Asian fusion. They appreciate good

Table 5. Experiments assessing decoder quality.

Data	Amazon-books			Yelp		
	P	R	F1	P	R	F1
Euclidean	0.3266	0.2854	0.3064	0.3511	0.2238	0.2872
Hyperbolic	0.3498	0.3009	0.3257	0.3608	0.2398	0.3021
Ours	0.3665	0.3167	0.3418	0.3716	0.2453	0.3081

food, drinks, and a relaxed atmosphere. They also value quality and freshness in their food.

In this example, the profile recovered by our decoder accurately captures the user’s preferences for Thai and Chinese cuisines, broadly summarized as an affinity for Asian fusion flavours. Additionally, our decoder identifies the user’s interest in diverse culinary experiences, indicating a propensity toward exploration.

Original item profile:

Ceol Irish Pub in Reno is a popular bar and pub known for its happy hour deals, great service, and friendly atmosphere. It is suitable for those who enjoy trivia nights, live music, and a wide selection of drinks, particularly whiskey. The pub has a welcoming environment, with bartenders who are attentive and quick to serve.

Recovered item profile:

Users who enjoy a variety of beer options, live music, and a relaxed atmosphere would enjoy Ceol Irish Pub.

The alignment between the original and recovered item profiles shows that our decoder effectively captures key thematic elements of Ceol Irish Pub. The original profile emphasizes aspects such as happy hour, a wide selection of drinks, live music, and a welcoming atmosphere with attentive service. The recovered profile distills these characteristics, focusing on the pub’s appeal for users who enjoy diverse beer options, live music, and a relaxed setting. This alignment suggests that our decoder reliably summarizes key attributes, albeit with a degree of abstraction.

C. Hierarchical Structure Case Study

In this section, we present a case study examining the exploration-exploitation trade-off in the hyperbolic hierarchical structure. We randomly select a user and identify items that share different layers of the lowest common ancestor (LCA) with the user in the hierarchy tree. Ideally, a larger LCA layer indicates that the user and item were grouped earlier in the hierarchy, suggesting a stronger likelihood of interaction. Conversely, a smaller LCA layer implies that the user and item were grouped only after multiple iterations, indicating a weaker likelihood of interaction.

User Profile:

The user enjoys books with supernatural elements, horror and paranormal romance. They also appreciate fast-paced action and suspenseful thrillers with political intrigue and espionage. The user likes complex characters dealing with dark themes.

Item 1 Profile (LCA=10):

The book 'Spirit Fighter (Son of Angels, Jonah Stone)' would likely appeal to young readers who enjoy stories about supernatural beings and the fight between good and evil. It is a book that offers entertainment and inspiration, as well as a glimpse into the supernatural world.

Item 2 Profile (LCA=5):

Fans of contemporary romance novels will enjoy Barefoot Summer (A Chapel Springs Romance). This book combines heartwarming romance, relatable heartaches, and lighthearted humor to create a delightful and engaging story. It is ideal for those looking for an easy-to-read and entertaining summer novel.

As demonstrated in the case study, the user shows a preference for supernatural elements, which aligns closely with the description of item 1, indicating a high likelihood of interaction. In contrast, while the user profile mentions a preference for dark themes, item 2 focuses on romance and heartwarming narratives, suggesting a low probability of user interest in item 2.

This analysis aligns seamlessly with the intended design of our hierarchical tree, further validating the effectiveness of our model in capturing and leveraging nuanced user-item relationships.